Sfp1 regulates transcriptional networks driving cell growth and division through multiple promoter binding modes

Benjamin Albert[1], Susanna Tomassetti[1], Yvonne Gloor, Daniel Dilg, Stefano Mattarocci, Slawomir Kubik and David Shore[*]

Department of Molecular Biology and Institute for Genetics and Genomics in Geneva (iGE3), 30 quai Ernest-Ansermet, 1211 Geneva 4, Switzerland

[1]These authors contributed equally to this work

[*]Corresponding author: David.Shore@unige.ch

Abstract

Understanding how transcriptional programs help to coordinate cell growth and division is an important unresolved problem. Here we report that the nutrient- and stress-regulated transcription factor Sfp1 is rate-limiting for expression of several large classes of genes involved in yeast cell growth, including ribosomal protein, ribosome biogenesis, and snoRNA genes. Remarkably, the spectrum of Sfp1 transcription effects is concordant with a combination of chromatin immunoprecipitation and chromatin endogenous cleavage binding analyses, which together provide evidence for two distinct modes of Sfp1 promoter binding, one requiring a co-factor and the other a specific DNA-recognition motif. In addition to growth-related genes, Sfp1 binds to and regulates the promoters of cell cycle "START" regulon genes, including the key G1/S cyclins *CLN1* and *CLN2*. Our findings suggest that Sfp1 acts as a master regulator of cell growth and cell size by coordinating the expression of genes implicated in mass accumulation and cell division.

Introduction

The expression of genes required for ribosome production is an intensive transcriptional process in growing cells (Warner, 1999) and serves as a paradigm to study coordination of large gene networks (Lempiainen & Shore, 2009). Regulation of ribosome production at the transcriptional level in eukaryotes is best understood in the budding yeast *Saccharomyces cerevisiae*, where RNA polymerase II (RNAPII)-mediated transcription of ribosomal protein (RP) genes, the suite of >200 protein-coding genes required for ribosome assembly (referred to as ribosome biogenesis [RiBi] genes), and small nucleolar RNA (snoRNA) genes is highly coordinated and regulated according to nutrient availability and stress. Despite this fact, the promoters of these three groups of genes are organized differently, begging the question of how they can be coordinately regulated (Bosio, Negri et al., 2011).

The Split-Finger Protein 1 (Sfp1) (Blumberg & Silver, 1991) is a nutrient- and stress-sensitive transcription factor (TF) that has emerged as a potential coordinator of cell growth and division. Deletion or over-expression of *SFP1* influences expression of a large number of genes related to growth, including RP and RiBi genes (Fingerman, Nagaraj et al., 2003, Jorgensen, Rupes et al., 2004, Marion, Regev et al., 2004). Consistent with a direct role in cell growth, Sfp1 is concentrated in the nucleus under optimal growth conditions, but rapidly relocates to the cytoplasm in response to nutrient deprivation or other stress conditions (Jorgensen et al., 2004, Marion et al., 2004). In addition to its role in cell growth, cellular levels of Sfp1 also influence cell size and cell-cycle progression (Cipollina, Alberghina et al., 2005, Jorgensen, Nishikawa et al., 2002, Xu & Norris, 1998). Thus, *sfp1Δ* cells are amongst the smallest viable single-gene deletion mutants, whereas *SFP1* overexpression leads to a large-cell phenotype (Jorgensen et al., 2002). Taken together, these findings suggest that Sfp1 might play a key role in coordinating cell growth and cell division. Interestingly, the transcriptional and cell-size phenotypes of *SFP1* are notably similar to those of the c-Myc proto-oncogene (Jorgensen et al., 2004, Jorgensen & Tyers, 2004, Lempiainen & Shore, 2009).

One paradox that has limited our understanding of Sfp1's mechanism of action is that the protein has been detected by Chromatin Immuno-Precipitation (ChIP) at only a small fraction of the promoters that it appears to regulate. For example, although ChIP detects Sfp1 at many RP gene promoters (Reja, Vinayachandran et al., 2015), it is undetectable at virtually all of the >200 RiBi gene promoters where

57 over-expression studies suggest that it might be a direct activator (Jorgensen et al., 2002, Jorgensen et
58 al., 2004).

59 Here we vastly expand our knowledge of Sfp1 binding by Chromatin Endogenous Cleavage (ChEC)-seq
60 analysis (Schmid, Durussel et al., 2004, Zentner, Kasinathan et al., 2015). Remarkably, we find that
61 ChEC and ChIP provide a highly complementary picture of Sfp1 binding, with distinct sets of sites
62 identified by one technique or the other. Our combined analysis provides evidence that Sfp1 directly
63 orchestrates TATA-binding protein (TBP) and RNAPII recruitment at a broad array of genes that drive
64 cell growth, including most RiBi, RP and snoRNA genes. In addition, we find that Sfp1 binds to the
65 promoters of many G1/S ("START") regulon genes that are targeted by the TF Swi4. Interestingly, Sfp1
66 binding sites identified by ChEC are enriched for the motif gAAAATTTTc, whereas binding identified by
67 ChIP is often strongly dependent on another TF: Ifh1 at RP genes or Swi4 at G1/S regulon genes. These
68 findings provide an unprecedented example of how the combination of ChIP and ChEC can reveal a
69 more complete picture of TF-chromatin interactions. Taken together, our results support a role for
70 Sfp1 as a master regulator that helps to orchestrate cell growth by coordinating transcriptional
71 programs involved in mass accumulation and cell division.

72 **Results**

73 ***Modulation of Sfp1 protein level triggers a genome-wide redistribution of RNAPII***

74 Steady-state mRNA measurements in strains deleted for *SFP1* have revealed up- or down-regulation of
75 more than 2000 genes (Cipollina et al., 2005, Cipollina, van den Brink et al., 2008, Jorgensen et al.,
76 2004). However, *sfp1Δ* cells grow very slowly, making it difficult to distinguish between direct and
77 indirect effects (O'Duibhir, Lijnzaad et al., 2014). Furthermore, measurements of steady-state mRNA
78 levels can mask transcription effects that are buffered by compensatory mRNA stability changes (Sun,
79 Schwalb et al., 2012). Therefore, to understand better the role of Sfp1 we decided to use RNAPII
80 occupancy measured by ChIP as a read-out for transcription, first examining the effect of Sfp1
81 overexpression. We placed *SFP1* under the control of a strong inducible promoter (p*GAL1*) and
82 measured RNAPII recruitment by ChIP-seq of the Ser5-phosphorylated form of RNAPII after 1h of
83 galactose induction. Sfp1 overexpression triggered a massive change in the transcriptional program,

84 consistent with previous findings (Jorgensen et al., 2004), with 745 genes up-regulated and 1429 genes
85 apparently down-regulated by at least 1.5-fold (**Figure 1A;** see **Table S1** for a complete list).

86 We were struck by the fact that many of the genes down-regulated upon Sfp1 overexpression are
87 glucose-repressed genes implicated in carbohydrate metabolism, whereas induced genes are strongly
88 enriched in RP and RiBi genes, as well as translation-related genes and genes associated with "non-
89 coding RNA metabolic processes" (see **Table S1** for GO term analysis). This global change in the
90 transcriptional program appears similar to that observed following glucose addition to cells growing on
91 less optimal carbon sources. To assess this resemblance more directly, we performed ChIP-seq of

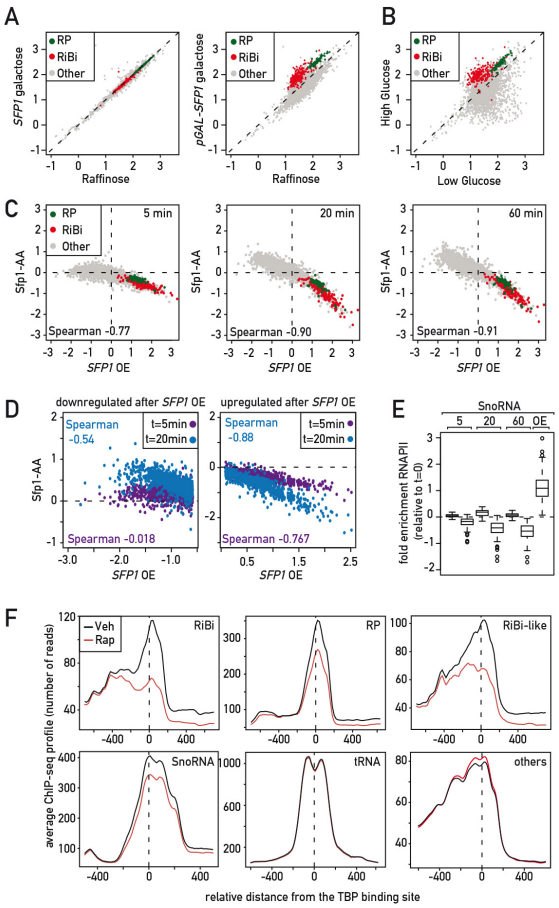

Figure 1: Regulation of growth-related genes by Sfp1. (A) Scatter plot comparing Rpb1 ChIP-Seq signal (log10 normalized read counts) in SFP1 (left panel) and pGAL1-SFP1 (right panel) strains grown in 2% raffinose (x-axis) or one hour following 2% galactose addition (y-axis). RP genes are indicated in green, RiBi genes in red and all other genes in grey. (B) Scatter plot, as in (A), comparing Rpb1 ChIP-Seq signal in low glucose (0.5%; x-axis) and 10 minutes after glucose addition to 2% (y-axis). (C) Scatter plots comparing Rpb1 ChIP-seq fold change (log2) relative to t=0 in a Sfp1-FRB anchor-away strain 5 (left panel), 20 (middle panel) and 60 (right panel) min following rapamycin addition (y axes) to Rpb1 ChIP-seq change relative to t=0 at 60 min following galactose addition in a pGAL-SFP1 strain (x-axes). RP and RiBi genes indicated as in (A). (D) Scatter plots derived from data shown in (C) in which genes down-regulated (left panel) and up-regulated (right panel) under conditions of SFP1 overexpression (x-axis) are compared to the effects at 5 min (purple) and 20 min (blue) following initiation of Sfp1 nuclear depletion (rapamycin addition). The Spearman correlation is indicated for each of the four separate categories. (E) Box plots showing Rpb1 ChIP-seq fold-change (log2) at snoRNA genes relative to t=0 for cells treated for 5, 20 or 60 min with rapamycin (red) or vehicle (grey) in a Sfp1 anchor-away strain (Sfp1-FRB), or 60 minutes following galactose addition to pGAL1-SFP1 cells (SFP1 OE). (F) Average TBP ChIP-seq signal centred on the TBP binding site at promoters of RiBi, RP, RiBi-like, snoRNA, tRNA, and all other genes (as indicated) 20 minutes following rapamycin (red) or vehicle (black) treatment of an Sfp1-FRB anchor-away strain.

92 RNAPII 10 minutes after a glucose pulse. We found a strong overlap between genes that are repressed
93 or activated in both conditions, including RiBi and RP genes (**Figure 1B** and **Figure S1A**). Consistent with
94 this finding, motifs identified in the promoters of genes up-regulated by Sfp1 over-expression are highly
95 similar to those up-regulated following a glucose pulse (**Figure S1B**). These data show that Sfp1 levels

96 can influence expression of more than one third of RNAPII-transcribed genes, suggesting that Sfp1
97 could play a key role in a much larger transcriptional network than is revealed by ChIP analysis of its
98 binding sites (Reja et al., 2015).

99 To challenge this idea, we used the "anchor-away" system (Haruki, Nishikawa et al., 2008) to measure
100 the immediate effect of rapid Sfp1 nuclear depletion on RNAPII association genome-wide. As expected,
101 nuclear depletion of Sfp1 causes a growth defect (**Figure S1C**). Strikingly, nuclear depletion of Sfp1 in
102 the anchor-away strain appears complete by ~15 minutes (**Figure S1D**), similar to what is observed in
103 wild-type strains following stress, inactivation of TORC1, or glucose depletion (Jorgensen et al., 2004).
104 To ascertain which genes might be direct targets of Sfp1, we measured RNAPII binding by ChIP-seq at
105 5, 20, and 60 minutes following rapamycin addition to the anchor-away strain and compared these data
106 to the changes observed following Sfp1 over-expression (1 hr growth of the *pGAL-SFP1* strain in
107 galactose; **Figure 1C**). We observed a significant anti-correlation between depletion and over-
108 expression effects (Spearman= 0.77, 0.90. and 0.91 after 5, 20 and 60 min, respectively, of rapamycin
109 treatment) confirming that the majority of up-regulated and down-regulated genes identified by over-
110 expression analysis are also sensitive to a reduction of Sfp1 nuclear levels. The weaker anti-correlation
111 at 5 minutes, compared to 20 or 60 minutes, results largely from those genes that appear to be
112 negatively regulated by Sfp1 (**Figure 1D**), suggesting that for at least some of these genes the inhibitory
113 effect of Sfp1 might be a secondary effect or that mechanisms by which Sfp1 directly inhibits expression
114 might follow slower kinetics than those by which it works as an activator. Since negative regulation
115 (direct or indirect) by Sfp1 was unanticipated, we performed a "spike-in" control (Chen, Hu et al., 2015),
116 using *Schizosaccharomyces pombe* chromatin (Bruzzone, Grunberg et al., 2018, Hu, Petela et al., 2015),
117 which allowed us to confirm that the increases observed in RNAPII binding following Sfp1 depletion
118 were not due to a normalization error in the ChIP-seq analysis.

119 ***Sfp1 promotes PIC assembly and transcription initiation at many growth-related genes***

120 We next analyzed in more detail the molecular roles of the genes that are both up-regulated after Sfp1
121 overexpression and down-regulated at 5, 20, and 60 minutes of depletion by >1.5-fold, i.e. those genes
122 where Sfp1 appears to be a direct activator. As indicated above, this group of over 500 genes is highly

123 over-represented by RiBi (201) and RP (112) genes (**Table S2**). Although both sets of genes are down-
124 regulated with similar kinetics following Sfp1 depletion, the magnitude of the effect is greater for RiBi
125 genes (**Figure S1E**). Other genes in this group display kinetics and amplitude of down-regulation most
126 similar to that of RiBi genes (**Figure S1G**), and analysis of their promoters reveals a strong enrichment
127 for the RRPE motif, and to a lesser extent the PAC motif, both of which are common to RiBi genes
128 (**Figure S1F**; (Bosio et al., 2011, Hughes, Estep et al., 2000)). In addition, many of these genes share
129 several functional annotations with RiBi genes (see **Table S2** for a complete list with GO terms), and we
130 thus refer to this group as "RiBi-like".

131 A more thorough examination of the novel Sfp1 target genes within the RiBi-like group revealed three
132 different connections to functions previously associated with Sfp1. First, we noted a strong enrichment
133 for genes involved in nuclear transport in the RiBi-like group, consistent with the initial identification of
134 *SFP1* based on a phenotype of altered nuclear import when present in multiple copies ((Blumberg &
135 Silver, 1991), see **Table S2**). Second, the RiBi-like group includes all known genes encoding proteins
136 involved in translation termination (**Table S3**), among which are the ribosome-associated Hsp70-like
137 proteins Ssb1/2, and the termination factors Sup45 and Sup35, all of which have also been directly
138 implicated in prion formation in yeast (Liebman & Chernoff, 2012). Curiously, Sfp1 also exists in a prion-
139 like form [*ISP*$^+$] that suppresses the phenotype of the prion-like derivative of Sup35 [*PSI*$^+$], perhaps by
140 increasing activation of genes linked to translation termination, and thus promoting translation
141 efficiency (Matveenko, Drozdova et al., 2016, Rogoza, Goginashvili et al., 2010, Volkov, Aksenova et al.,
142 2002). Finally, we also identified new Sfp1 target genes with regulatory functions connected to Sfp1.
143 One of these, *MRS6*, encodes the only yeast Rab escort protein, which in addition to its essential
144 function in secretion, interacts directly with Sfp1 and regulates its nuclear localization (Lempiainen,
145 Uotila et al., 2009, Singh & Tyers, 2009). Another novel target of Sfp1, *TOD6*, encodes a repressor of
146 RiBi genes (Huber, French et al., 2011, Lippman & Broach, 2009). These regulatory links point to
147 possible feedback mechanisms that might act to fine-tune nutrient and/or stress responses.

148 We then asked whether Sfp1 could be involved in transcription of snoRNA genes, a distinct set of RiBi-
149 like genes many of whose promoters are bound by Tbf1 and Reb1, two essential general regulatory
150 factors (Bosio et al., 2011, Preti, Ribeyre et al., 2010). Transcription of most of the 78 snoRNA genes is

151 driven by a dedicated RNAPII promoter comprising an individual transcription unit (59 genes), whereas
152 some are grouped in operons and a few are embedded within introns of either RP or RiBi genes (Bosio
153 et al., 2011). Notably, snoRNA genes as a whole display significant down-regulation following Sfp1
154 depletion and marked up-regulation upon Sfp1 over-expression, similar to that of RiBi, RP, and RiBi-like
155 genes (**Figure 1E**).

156 To investigate how Sfp1 impacts transcription, we first asked whether it influences pre-initiation
157 complex (PIC) assembly, the first step in RNAPII recruitment, by monitoring TBP binding. Indeed, rapid
158 nuclear depletion of Sfp1 leads to a significant drop in TBP ChIP-seq signal that tracks with the RNAPII
159 decrease (i.e. larger at RiBi and RiBi-like genes, compared to RP and snoRNA genes; **Figure 1F**). As
160 expected, Sfp1 depletion has no effect on TBP binding at genes where RNAPII recruitment is unaffected,
161 or at RNAPIII-transcribed tRNA genes. Since Sfp1 has been suggested to affect RNAPII processivity,
162 particularly at RP genes (Gomez-Herreros, de Miguel-Jimenez et al., 2012), we quantified the RNAPII
163 distribution across ORFs following Sfp1 depletion but found no change (**Figure S1H**).

164 ***ChIP-seq reveals dynamic carbon source-related binding of Sfp1 at G1/S network genes***

165 To determine if Sfp1 acts directly at the promoters of the genes described above we performed a ChIP-
166 seq experiment with a strain expressing a Sfp1-TAP fusion protein from the endogenous *SFP1* locus.
167 Given the fact that *sfp1Δ* most strongly impairs growth in medium containing glucose as carbon source,
168 we decided to measure Sfp1 binding in three different carbon source conditions (glucose and two
169 "poor" carbon sources, raffinose and galactose). As reported previously (Fingerman et al., 2003,
170 Jorgensen et al., 2002, Marion et al., 2004, Reja et al., 2015), Sfp1 promoter binding at many RP genes
171 is observed in glucose-grown cells, but few if any binding events are detected at RiBi genes under these
172 conditions. We also observed robust Sfp1 binding at RP gene promoters in cells grown in either
173 galactose or raffinose (**Table S4**). However, we identified ~100 target genes in glucose-grown cells that
174 scored negative in both galactose and raffinose when we applied a conservative cut-off for specific

175 binding events (see **Figure 2A** for one example, **Figure S2A, Table S4**).A quantitative analysis of Sfp1

176 binding at promoters of these genes showed that binding is not absent in sub-optimal carbon sources

177 but is instead decreased by about 1.5- to 3-fold compared to that in glucose (**Figure 2B).** Strikingly, we

178 found that the group of genes where Sfp1 binding is glucose-enhanced is highly enriched in genes

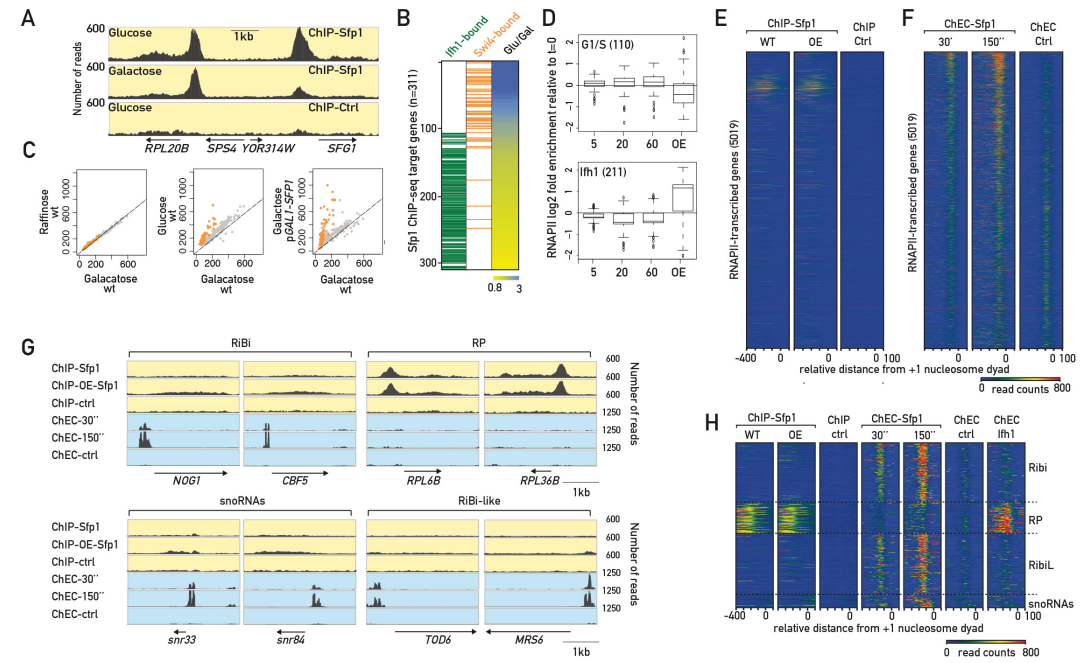

Figure 2: ChIP and ChEC detect distinct classes of Sfp1 promoter binding sites (A) Genome browser tracks comparing Sfp1-TAP ChIP-seq signals in glucose or galactose medium, or in an untagged strain grown in glucose. The position and direction of transcription of individual genes is shown below. (B) Heat map showing ratio of Sfp1-TAP ChIP-seq signal from glucose-grown versus galactose-grown cells. Genes whose promoters are bound by Swi4 (Harbison, Gordon et al., 2004) or Ifh1 (Knight, Kubik et al., 2014) are indicated in orange or green, respectively. (C) Scatter plots comparing Sfp1-TAP ChIP-seq signal in a *SFP1-TAP* strain (WT) grown in galactose (x-axis) with signal in raffinose (left pane, y-axisl), glucose (middle panel, y-axis) or with a *pGAL1-SFP1-TAP* strain after 60 minutes growth in galactose (right panel, y-axis). Promoter of genes whose Sfp1 binding increases more than 1.5-fold are indicated in orange. (D) Box plots showing Rpb1 ChIP-seq fold-change (log2) at genes where Sfp1 promoter binding changes according to carbon source ("G1/S", top panel) or where Sfp1 promoter binding is detected in all carbon sources tested ("Ifh1", bottom panel). (E) Heat maps showing Sfp1-TAP ChIP-seq signal in a SFP1-TAP strain (WT) or a pGAL1-SFP1-TAP strain (over-expression, OE) after 60 minutes growth in galactose. ChIP-seq in an untagged strain (ctrl) is shown to the right. Rows (y-axis) consist of 5019 RNAPII-transcribed genes with a well-defined +1 nucleosome, ordered according to decreasing RNAPII fold-change after 5 minutes of rapamycin treatment in a Sfp1-FRB anchor-away strain (top to bottom). Signal densities from -400 to +100 bp relative to the +1-nucleosome dyad axis are shown (x-axis). (F) Heat maps showing Sfp1-MNase or free MNase (ctrl) ChEC-seq signal at the indicated times following calcium treatment. Genes (rows on y-axis) and signal density relative to TSS (x-axis) are as in (E). (G) Genome browser tracks comparing Sfp1-TAP or untagged ChIP-seq signals (yellow background) to Sfp1-MNase and free MNase ChEC-seq signals (blue background), the latter at the indicated time points following calcium addition. The position and direction of transcription of individual genes is shown below. (H) Heat maps showing Sfp1-TAP ChIP-seq under endogenous expression (WT) or after over-expression of Sfp1 (OE), Sfp1 ChEC-seq signal after 30 or 150 seconds of calcium treatment, and Ifh1 ChEC-seq signal after 150 seconds of calcium treatment in a window of 500 bp containing +1 nucleosome (0) at different categories of genes. Control for ChIP (untagged strain) or ChEC (free-MNase) are also shown.

179 implicated in the G1/S cell-cycle transition, or "START" ((Bertoli, Skotheim et al., 2013); **Figure 2B, Table**

180 **S4**), whose promoters are typically bound by the Swi4 activator. In contrast, genes where Sfp1

181 promoter binding was essentially equivalent in all carbon sources were highly enriched in Ifh1-bound
182 RP genes.

183 To reveal if this glucose-specific increase of Sfp1 promoter binding is linked to its nuclear concentration,
184 which is known to change according to growth conditions (Jorgensen et al., 2004), we determined
185 whether increasing total levels of Sfp1 by growing *pGAL1-SFP1* cells in galactose could be sufficient to
186 recapitulate the binding pattern of Sfp1 observed in glucose. Remarkably, Sfp1 overexpression
187 specifically increased Sfp1 promoter binding at glucose-sensitive promoters but not at those binding
188 sites common to all three carbon sources (**Figure 2C**). These data suggest that Sfp1 binding, specifically
189 at G1/S gene network promoters, is limited by Sfp1 concentration or activity when cells are grown in
190 the presence of a sub-optimal (non-glucose) carbon source.

191 To examine the function of Sfp1 at the START-specific group of genes, we quantified RNAPII association
192 by Rbp1 ChIP-seq following both Sfp1 nuclear depletion and over-expression. In contrast to what we
193 observed at other gene groups, Sfp1 over-expression led to a decrease in RNAPII binding at most START-
194 specific genes, and its depletion caused a slight increase in average RNAPII binding, suggesting that Sfp1
195 may act as a negative regulator at many of these genes (**Figure 2D**). Interestingly, Sfp1 has been
196 described as a negative regulator of START not only due to its ability to promote ribosome biogenesis
197 and growth, but also through an unknown mechanism acting at the level of *CLN1/2* transcription, which
198 drives the G1/S transition ((Aldea, Jenkins et al., 2017, Ferrezuelo, Colomina et al., 2012); see below).

199 ***ChEC-seq reveals Sfp1 target genes that are missed by ChIP***

200 Although the ChIP-seq experiments described above confirmed Sfp1 binding to a number of genes
201 where functional experiments suggest it is either a positive or negative regulator, they fail to explain
202 how Sfp1 controls expression of large groups of additional target genes, such as RiBi, RiBi-like and
203 snoRNA genes. We thus asked whether an alternative assay to measure TF binding, chromatin
204 endogenous cleavage (ChEC; (Schmid et al., 2004)), could reveal Sfp1 binding at the promoters of these
205 genes. To this end, we fused the gene encoding micrococcal nuclease (MNase) to the C-terminus of
206 the endogenous *SFP1* gene and performed a ChEC assay, results of which were analyzed by high
207 throughput sequencing (ChEC-seq; (Zentner et al., 2015)). Strikingly, this revealed a strong signal, well

208 above a background observed after prolonged digestion in a strain expressing free MNase, at a much
209 larger number of promoters than was detected by Sfp1-TAP ChIP-seq (**Figure 2E, 2F, Table S5**).
210 Significantly, target genes identified by ChEC-seq share similar functional annotations with genes that
211 we identified above, using functional assays, as targets of Sfp1 (**Table S5**). In fact, the magnitude of the
212 Sfp1-MNase ChEC-seq signal at promoters correlated much better than that of Sfp1-TAP ChIP-seq with
213 the transcriptional effect observed upon Sfp1 nuclear depletion (**Figure 2E 2F, S2C**).

214 To examine the Sfp1 ChEC-seq results in more detail, and better compare them to those obtained by
215 ChIP-seq, we focused on the group of over 500 genes described above, whose expression is most
216 strongly dependent upon Sfp1. As before, we divided this group of genes into four sub-groups: the RiBi
217 factors (as defined by Jorgensen et al. (2004)), the RP genes, the "RiBi-like" genes and the snoRNA
218 genes. Mapping both Sfp1 ChIP-seq and Sfp1 ChEC-seq signals on these separate groups (**Figure 2H**
219 **and S2D**) shows clearly that ChIP-seq reveals Sfp1 binding at RP genes, but little or no binding at RiBi,
220 RiBi-like, or snoRNA genes. The opposite is true for ChEC-seq. Genome browser screen shots of specific
221 examples of this effect are shown in **Figures 2G** and **S2B**.

222 This complementary behaviour of Sfp1 is not a universal feature of the ChEC assay as applied to TFs,
223 since the ChEC-seq results for three general regulatory factors in yeast (Rap1, Abf1 and Reb1) are largely
224 concordant with those obtained by ChIP (Zentner et al., 2015). We also find that Ifh1 ChEC analysis
225 yields a profile very similar to that of ChIP (strong cleavage almost exclusively at RP genes; **Figure 2H**).
226 Nevertheless, we have no reason to believe that the differential behaviour of Sfp1 in these two
227 chromatin binding assays is unique to this factor.

228 ***Co-factor dependent and sequence-driven binding modes of Sfp1***

229 In considering possible causes for the different behaviour of Sfp1 in ChEC and ChIP assays, we first
230 noted that most RP gene promoters, in addition to being bound by the general regulatory factor Rap1,
231 are also bound by a highly RP gene-specific set of co-activator proteins, Fhl1 and Ifh1 (Jorgensen et al.,
232 2004, Martin, Soulard et al., 2004, Rudra, Zhao et al., 2005, Schawalder, Kabani et al., 2004, Wade, Hall
233 et al., 2004). In contrast, RiBi genes have not been associated with any specific activator protein(s).

234 Since Ifh1 binding is co-incident with that of Sfp1 at RP genes (**Figure 3A**), we wondered whether Sfp1
235 association at these genes might be dependent on this factor. To test this idea, we measured Sfp1
236 binding at two RP genes following rapid nuclear depletion of Ifh1 and found that it is strongly reduced
237 under these conditions (**Figure 3B**). This dependence upon Ifh1 for Sfp1 binding probably extends to

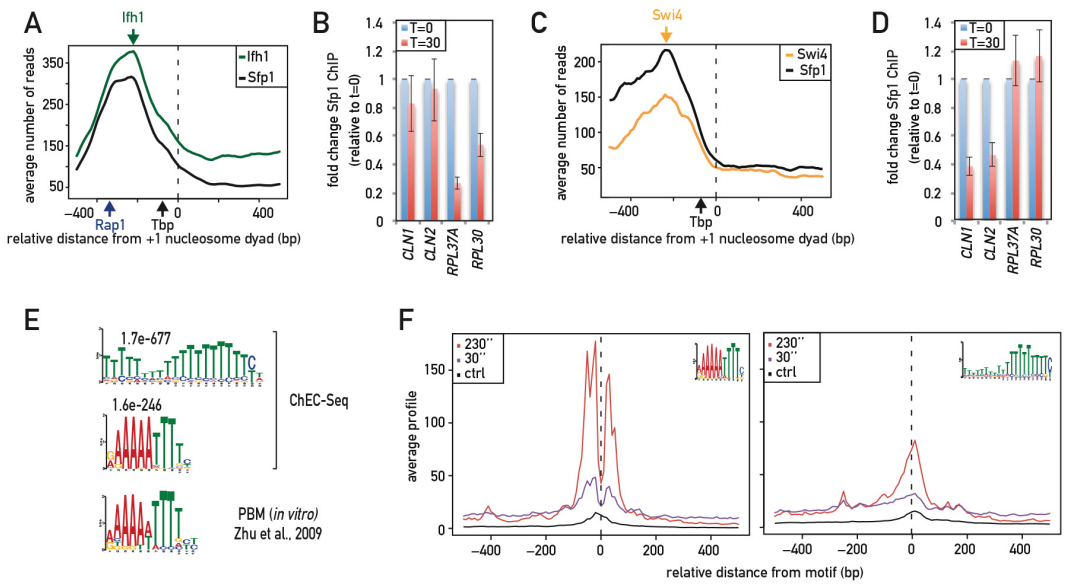

Figure 3: Co-factor-dependent and DNA sequence motif-dependent modes of Sfp1 binding. (A) Average ChIP-seq signal of Ifh1-Myc (green) and Sfp1-TAP (black) occupancy at RP genes, centred on the position of the +1 nucleosome. Blue and black arrows show average positions of Rap1 and TBP binding, respectively. (B) Sfp1 occupancy (qPCR-ChIP) at the *CLN1, CLN2, RPL30* and *RPL37A* promoters for the indicated times following auxin treatment in a Ifh1-AID strain; fold enrichment relative to *ACT1* was normalized to values at t = 0, which were set to 1. (C) Average ChIP-seq signal of Swi4 (green) and Sfp1-TAP (black) occupancy at Swi4 regulated genes identified in ChIP-seq of Sfp1, centred on the position of the +1 nucleosome. Black arrows show average positions of TBP binding. (D) Sfp1 occupancy (qPCR-ChIP) at the *CLN1, CLN2, RPL30* and *RPL37A* promoters at the indicated time following rapamycin treatment in a Swi4-FRB strain; fold enrichment relative to *ACT1* was normalized to values at t = 0, which were set to 1. (E) Motif enrichment identified by MEME analysis of sequences centred on Sfp1-ChEC peaks or by in vitro protein-binding microarray (PBM) analysis (Zhu, Byers et al., 2009), as indicated. (F) Average plots of Sfp1 cleavage around the indicated motifs (top right of each panel) enriched in Sfp1-ChEC (30 or 150 seconds after Ca^{+2} addition). Control averages (free-MNase cleavage 20 minutes after Ca^{+2}) at these sites is also shown. Center of motif is indicated by a vertical dotted line.

238 all RP genes, since we observe a very strong correlation between the ChIP-seq strength of the two
239 factors that is largely specific to these genes (**Figure S3A**). As noted above (**Fig. 2B**) many additional
240 Sfp1 promoter binding sites detected by ChIP are also bound by the TF Swi4, and at these promoters
241 we found that Sfp1 binding is highly coincident with that of Swi4 (**Figure 2C**). Anchor-away of Swi4
242 caused a strong decrease in Sfp1 binding at two such genes that we tested, those encoding the G1/S
243 cyclins Cln1 and Cln2 (**Figure 3D**). We thus infer that many of the Sfp1 binding events detected by ChIP
244 are linked to recruitment through another TF: Ifh1 at RP genes and Swi4 at G1/S regulon genes. These

245 would appear to explain the majority of ChIP-detectable binding events, though other examples may
246 exist where a different co-factor helps to recruit Sfp1.

247 To understand how Sfp1 is recruited at genes where it is detected by ChEC, we searched for a common
248 DNA feature near the sites of Sfp1-MNase cleavage (Bailey, 2011). We found a strong enrichment for
249 two different motifs, one a large stretch of A residues, the other a palindromic A/T-rich sequence that
250 strongly resembles the RiBi-associated RRPE motif (**Figure 3E**). These two motifs are also enriched at
251 promoters of genes that are affected by Sfp1 depletion or overexpression (**Figure S2B**), consistent with
252 the high correlation of these data sets. Significantly, protein-binding microarray (PBM) data indicate
253 that Sfp1 has DNA-binding specificity for an RRPE-like DNA sequence nearly identical to the palindromic
254 motif identified by our ChEC experiments (Zhu et al., 2009), suggesting that Sfp1 binds directly to this
255 motif in vivo. In contrast, the polyA motif is common to the three other yeast transcription factors
256 characterized to date in a pioneering ChEC study (Abf1, Reb1 and Rap1; (Zentner et al., 2015)) and has
257 been proposed to reflect a scanning mode DNA binding for these factors. We have not examined this
258 hypothesis further but would note that the Sfp1-MNase cleavage pattern surrounding the RRPE-like
259 motif is distinct from that seen at polyA tracts (**Figure 3F**) and suggestive of stable binding at the RRPE
260 motif and cutting on either side of the motif, as opposed to the broad observed cleavage across the
261 non-specific site (Zentner et al., 2015).

262 Discussion

263 Results described here help to clarify the previously enigmatic role of Sfp1 in transcription and directly
264 place this protein at the center of transcriptional networks controlling ribosome biogenesis and other
265 growth-promoting processes, as well as the G1 to S transition (START) (**Figure 4**). Although previous
266 studies indicated that Sfp1 is an activator of RiBi genes, this conclusion was based upon steady-state
267 mRNA measurements in an extremely slow growing *sfp1Δ* strain or upon *SFP1* overexpression. The
268 absence of a Sfp1 ChIP signal at RiBi genes thus raised serious concerns that its effect at these genes
269 might be indirect. Our findings put these concerns to rest by demonstrating robust association of Sfp1
270 with RiBi gene promoters, using ChEC-seq, and by revealing that rapid and acute Sfp1 nuclear depletion,

271 by anchor-away, results in immediate and strong down-regulation of these genes. We note at the same

272 time, though, that many genes, most of which are weakly expressed in normal growth conditions,

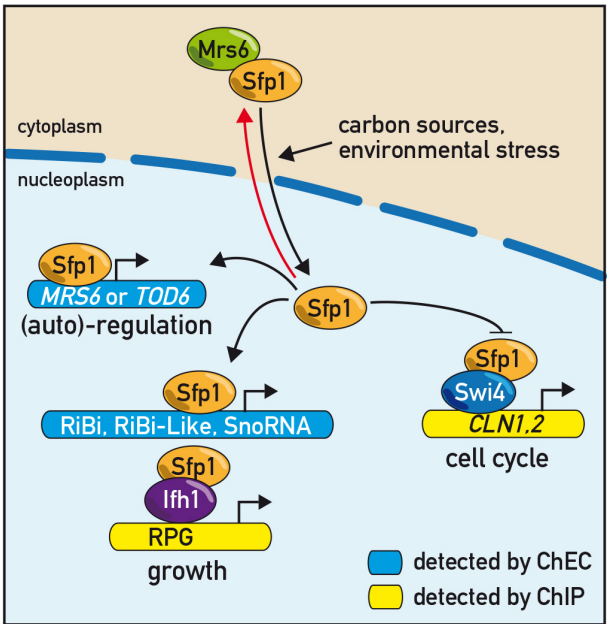

Figure 4: Schematic representation of Sfp1 binding and regulation. According to growth conditions Sfp1 shuttles between the nucleus and the cytoplasm allowing it to adjust TBP and RNAPII recruitment at a vast array of growth-related genes including RiBi, RiBi-like, snoRNA, and RP genes. Sfp1 also binds to and controls expression of its own regulator (*MRS6*) and that of the RiBi gene repressor *TOD6*, possibly to facilitate the rapid shut-down of growth-related transcription upon stress. Finally, Sfp1 is recruited at the promoters of START-specific genes, such as the two G1/S cyclin genes *CLN1* and *CLN2*, in a Swi4-dependent manner. The ability of Sfp1 to bind to and regulate a wide variety of promoter, places Sfp1 an ideal position to co-ordinately regulate cell growth and the commitment to cell division (START) at a transcriptional level.

273 appear to be negatively regulated by Sfp1, since their expression increases upon Sfp1 nuclear depletion

274 and decreases upon Sfp1 over-expression (**Fig. 1C, D**). Given that most of these Sfp1-repressed genes

275 show no evidence of Sfp1 promoter binding (*CLN1* and *CLN2* being notable counter-examples, see **Fig.**

276 **3D** and below), how can one explain this regulation? One possibility is that the massive down-

277 regulation of highly-transcribed genes upon Sfp1 nuclear depletion releases significant amounts of

278 RNAPII, and/or important general co-activators, that through mass action increase the expression of

279 many weakly transcribed genes where polymerase and co-activators might be limiting. This

280 explanation is consistent with the delayed effect of up-regulation upon Sfp1 withdrawal but remains to

281 be tested by future experiments.

282 Although Sfp1 has long been implicated in cell size determination, it has been unclear whether its role

283 is exclusively related to activation of ribosome biogenesis programs or if it also serves as a more direct

284 inhibitor of START (Aldea et al., 2017, Ferrezuelo et al., 2012, Jorgensen & Tyers, 2004). Our

285 identification of *CLN1* and *CLN2* as targets of negative regulation by Sfp1 is supports the latter

286 hypothesis and warrants further study. Although still speculative, we note that inhibition of *CLN1/2*

287 expression by Sfp1 would be expected to delay START and thus prolong growth before division occurs,

288 consistent with the observation that *sfp1Δ* cells are unusually small compared to WT cells. We also
289 note that the glucose-dependent binding of Sfp1 at *CLN1/2* promoters may explain their repression by
290 the cyclic AMP signaling pathway (Baroni, Monti et al., 1994, Tokiwa, Tyers et al., 1994), which is
291 activated by glucose addition to cells growing in poor carbon sources. Nevertheless, the association of
292 Sfp1 with a large number of other genes in the G1/S regulon raises the possibility that Sfp1 regulation
293 of START may extend well beyond its role in *CLN1/2* expression.

294 The application of ChEC-seq and related MNase-based methods ("Chromatin Immuno-Cleavage [ChIC]
295 (Schmid et al., 2004) or "Cleavage Under Targets and Release Using Nuclease" [CUT&RUN] (Skene &
296 Henikoff, 2015)) is still in its infancy. Nevertheless, we are unaware of other cases, as described here
297 for Sfp1, where ChIP and in vivo MNase-cleavage methods yield such contrasting results. Significantly,
298 both ChIP and ChEC for Sfp1 are concordant with functional data (transcriptional changes upon
299 depletion or over-expression) even though each reports on only a subset of the Sfp1 regulatory
300 landscape. Our findings thus highlight limitations of both techniques for measuring chromatin
301 association of specific proteins, that may be under-appreciated. For example, the failure of ChIP to
302 detect Sfp1 binding at RiBi and RiBi-like genes would appear surprising considering our evidence that
303 these interactions result from direct DNA binding. One possible explanation for this discrepancy is that
304 the proposed Sfp1 binding motif, the RRPE element, is extremely A/T-rich and may thus be unable to
305 form direct cross-links with Sfp1 at a detectable frequency (Rossi, Lai et al., 2018). Alternatively, or in
306 addition, the C-terminal epitope tags so far used to detect Sfp1 by ChIP may be masked at sites where
307 Sfp1 binds directly to DNA, but not at those sites where its binding is dependent upon a second TF. In
308 the case of ChEC, we imagine that Sfp1 detection at RP and G1/S regulon genes might be limited by a
309 short binding half-life and/or access of the tethered MNase to accessible promoter DNA. We suggest
310 that the pleiotropic chromatin-binding behavior of Sfp1 described here is not unique and propose that
311 the complementary application of ChEC-seq and related techniques maybe be essential for identifying
312 the full spectrum of TF targets, not just in yeast, but also in more complex metazoan organisms.

313

314 # Methods

315 ***Yeast strains***

316 A complete list of all strains used in this study is provided in the Supplementary Tables 6. Strains were
317 generated by genomic integration of tagging or disruption cassettes (Longtine, McKenzie et al., 1998,
318 Rigaut, Shevchenko et al., 1999).

319 ***Yeast growth conditions***

320 Experiments were performed with log phase cells harvested between OD_{600} 0.4 and 0.6. Yeast strains
321 used in this study are listed in Table 6. Overnight cultures were diluted to OD_{600} = 0.1, grown at 30°C
322 to exponential phase (OD_{600} = 0.4), and then treated with rapamycin at 1µg/ml (from a 1 mM stock
323 solution in 90% ethanol, 10% Tween-20) for anchor-away experiments. Genome-wide localization of
324 Sfp1-TAP was analyzed under standard growth conditions in YP Galactose 2%, Raffinose 2% or Glucose
325 2%, and the untagged wild type (WT) strain (YDS2) was used as a control. The strain expressing *pGAL1-*
326 *SFP1-TAP* was grown in raffinose-containing medium for two generations and subsequently treated for
327 1 hr with 2% galactose to induce *SFP1* expression. For glucose pulse experiments, WT strains were
328 grown in YP glycerol (3%), glucose (0.05%) and shifted to yeast extract, peptone, adenine, and dextrose
329 medium (YPAD; 2% glucose).

330 ***Yeast growth assays***

331 Yeast strains were grown in the appropriate medium to a concentration of 1×10^7 cells/ml. Serial 10-
332 fold dilutions were spotted either on YPAD plates or on plates containing selective medium, at the
333 indicated temperature. Plates were photographed after 2 days of incubation unless otherwise noted.

334 ***Live cell microscopy***

335 All cultures for microscopy experiments were grown to early exponential phase in riboflavin-free
336 medium. Rapamycin was directly added to the cultures at a final concentration of 1 µg/ml. Images
337 were acquired using a wide-field fluorescence microscope (Zeiss Axio Imager Z1m) equipped with a CCD
338 camera.

339 ***ChIP-seq***

340 Cultures of 200 ml were collected at OD_{600} 0.5-0.8 for each condition. The cells were crosslinked with
341 1% formaldehyde for 10 min at room temperature and quenched by adding 125 mM glycine for 5 min
342 at RT. Cells were washed with ice-cold HBS and resuspended in 3.6 ml of ChIP lysis buffer (50 mM
343 HEPES-Na pH 7.5, 140 mM NaCl, 1mM EDTA, 1% NP-40, 0.1% sodium deoxycholate) supplemented with
344 1mM PMSF and 1x protease inhibitor cocktail (Roche). Samples were aliquoted in 6 Eppendorf tubes
345 and frozen. After thawing, the cells were broken using Zirconia/Silica beads (BioSpec). Lysates were
346 spun at 13'000 rpm for 30 min at 4°C. The pellet was resuspended in 300 µl ChIP lysis buffer + 1mM
347 PMSF and sonicated for 15 min (30" on - 60" off) in the Bioruptor (Diagenode). Sonicated lysates were
348 then spun at 7'000 rpm for 15 min at 4°C. Sfp1-TAP, RNAPII, and TBP-Myc binding were analyzed using
349 TAP-specific, Rpb1, and anti-Myc antibody, respectively (Thermo Fisher CAB1001 or Abcam 5131, Myc
350 epitope 9E10). The antibody (1 µg per 300 µl of lysate) was added to the supernatant and incubated
351 for 1h at 4°C. The magnetic beads were washed three times with PBS plus 0.5% BSA, added to the
352 lysates (30 µl of beads per 300 µl of lysate) and incubated for 2 hr at 4°C. The beads were then washed
353 twice with 50 mM HEPES-Na pH 7.5, 140 mM NaCl, 1mM EDTA, 0.03% SDS, once with AT2 buffer (50
354 mM HEPES-Na pH 7.5, 1 M NaCl, 1mM EDTA), once with AT3 buffer (20 mM Tris-Cl pH 7.5, 250 mM LiCl,
355 1mM EDTA, 0.5% NP-40, 0.5% sodium deoxycholate) and twice with TE. Chromatin was eluted from
356 the beads by resuspending in TE + 1% SDS and incubation at 65°C for 10 min. The eluate was transferred
357 to an Eppendorf tube and incubated overnight at 65 °C to reverse the crosslinks. DNA was purified
358 using the High Pure PCR Cleanup Micro Kit (Roche) and libraries were prepared for sequencing using
359 the TruSeq ChIP Sample Preparation Kit (Illumina) according to the manufacturer's instructions. The
360 libraries were sequenced on a HiSeq 2500 machine and the reads were mapped to the sacCer3 genome
361 assembly using HTSstation (David, Delafontaine et al., 2014).

362 ***Sfp1 binding***

363 ChIP-seq peaks of Sfp1 binding were defined by shifting the plus and minus strand ChIP-seq profiles
364 towards each other by 150 bp and extending each read by 40 bp. To quantify ChIP-seq signals for each
365 promoter, a ratio between the total number of reads from each sample in a 400 bp region upstream
366 the transcription start site (TSS; (Jiang & Pugh, 2009)) of each ORF and the total number of reads from

367 the same region obtained with mock IP of the control untagged strain. The same logic was applied to
368 quantify signals within ORFs.

369 ***Swi4 and Ifh1 binding***

370 ChIP data from Harbison et al. (2004) and Knight et al. (2014) were used to map Swi4 and Ifh1 binding,
371 respectively. The ChIP-seq peaks (Knight et al., 2014) were defined by shifting the plus and minus strand
372 ChIP-seq profiles towards each other by 150 bp and extending each read by 40 bp. To quantify ChIP-
373 seq signals for each promoter, the total number of reads from each sample in a 400 bp region upstream
374 the TSS (transcription start site; (Jiang & Pugh, 2009)) of each ORF was determined.

375 ***TBP binding***

376 ChIP-seq signals for TBP were quantified at (TBP binding site) positions taken from (Rhee & Pugh, 2012).

377 ***Rpb1 (RNAPII) binding***

378 To quantify Rpb1 ChIP-seq signals for each gene, a ratio was calculated of the total number of reads in
379 each ORF before treatment to the total number of reads in each ORF after the indicated times of
380 rapamycin or vehicle treatment, or after 1h in galactose for the strain carrying *pGAL1-SFP1-TAP*. In the
381 Sfp1-FRB anchor-away experiment measuring Rbp1 ChIP, *S. pombe* chromatin was used as a "spike-in"
382 control for normalization, as described previously (Bruzzone et al., 2018).

383 ***ChEC-seq***

384 ChEC-seq experiments were performed essentially as described (Zentner et al., 2015) with the following
385 modifications. Cells in which MNase was fused at the C-terminus of the endogenous *SFP1* gene were
386 used to determine Sfp1 binding. Cells in which MNase was placed under the control of *REB1* promoter
387 were used as a control. One sample corresponds to 12 ml of culture at OD_{600} = 0.7. Cells were washed
388 twice with buffer A (15 mM Tris 7.5, 80 mM KCl, 0.1 mM EGTA, 0.2 mM spermine, 0.5 mM spermidine,
389 1xRoche EDTA-free mini protease inhibitors, 1 mM PMSF) and resuspended in 200 µl of buffer A with
390 0.1% digitonin. The cells were incubated for 5 min at 30°C at which point MNase was induced by
391 addition of 5 mM $CaCl_2$ and stopped at the desired timepoint by adding EGTA to a final concentration
392 of 50 mM. DNA was purified using MasterPure Yeast DNA purification Kit (Epicentre) according to the

393 manufacturer's instruction. Large DNA fragments were removed by a 5-min incubation with 2.5x
394 volume of AMPure beads (Agencourt) after which the supernatant was kept, and MNase-digested DNA
395 was precipitated using isopropanol. Libraries were prepared using NEBNext kit (New England Biolabs)
396 according to the manufacturer's instructions. Before the PCR amplification of the libraries small DNA
397 fragments were selected by a 5-minute incubation with 0.9x volume of the AMPure beads after which
398 the supernatant was kept and incubated with the same volume of beads as before for another 5 min.
399 After washing the beads with 80% ethanol the DNA was eluted with 0.1x TE and PCR was performed.
400 Adaptor dimers were removed by a 5-min incubation with 0.8x volume of the AMPure beads after
401 which the supernatant was kept and incubated with 0.3x volume of the beads. The beads were then
402 washed twice with 80% ethanol and DNA was eluted using 0.1x TE. The quality of the libraries was
403 verified by running an aliquot on a 2% agarose gel. Libraries were sequenced using a HiSeq 2500
404 machine in single-end mode. Reads were extended by the read length. To analyze the Sfp1-MNase
405 binding pattern, read ends were considered to be MNase cuts and were mapped to the genome
406 (sacCer3 assembly) using HTSstation (David et al., 2014). For peak analysis MACS software was used
407 through HTSstation, using free-MNase signal as background. Motifs were detected using MEME (Bailey,
408 Boden et al., 2009) with sequences from each identified ChEC signal peak as input.

409 ***Data and software availability***

410 All sequencing and microarray data generated in this study were submitted to the GEO database as
411 SuperSeries GSE118561.

412

413 # References

414

415 Aldea M, Jenkins K, Csikasz-Nagy A (2017) Growth Rate as a Direct Regulator of the Start Network to
416 Set Cell Size. Front Cell Dev Biol 5: 57

417 Bailey TL (2011) DREME: motif discovery in transcription factor ChIP-seq data. Bioinformatics 27: 1653-
418 9

419 Bailey TL, Boden M, Buske FA, Frith M, Grant CE, Clementi L, Ren J, Li WW, Noble WS (2009) MEME
420 SUITE: tools for motif discovery and searching. Nucleic Acids Res 37: W202-8

421 Baroni MD, Monti P, Alberghina L (1994) Repression of growth-regulated G1 cyclin expression by cyclic
422 AMP in budding yeast. Nature 371: 339-342

423 Bertoli C, Skotheim JM, de Bruin RA (2013) Control of cell cycle transcription during G1 and S phases.
424 Nat Rev Mol Cell Biol 14: 518-28

425 Blumberg H, Silver P (1991) A split zinc-finger protein is required for normal yeast growth. Gene 107:
426 101-10

427 Bosio MC, Negri R, Dieci G (2011) Promoter architectures in the yeast ribosomal expression program.
428 Transcription 2: 71-77

429 Bruzzone MJ, Grunberg S, Kubik S, Zentner GE, Shore D (2018) Distinct patterns of histone
430 acetyltransferase and Mediator deployment at yeast protein-coding genes. Genes Dev

431 Chen K, Hu Z, Xia Z, Zhao D, Li W, Tyler JK (2015) The Overlooked Fact: Fundamental Need for Spike-In
432 Control for Virtually All Genome-Wide Analyses. Mol Cell Biol 36: 662-7

433 Cipollina C, Alberghina L, Porro D, Vai M (2005) SFP1 is involved in cell size modulation in respiro-
434 fermentative growth conditions. Yeast 22: 385-99

435 Cipollina C, van den Brink J, Daran-Lapujade P, Pronk JT, Vai M, de Winde JH (2008) Revisiting the role
436 of yeast Sfp1 in ribosome biogenesis and cell size control: a chemostat study. Microbiology
437 154: 337-46

438 David FP, Delafontaine J, Carat S, Ross FJ, Lefebvre G, Jarosz Y, Sinclair L, Noordermeer D, Rougemont
439 J, Leleu M (2014) HTSstation: a web application and open-access libraries for high-throughput
440 sequencing data analysis. PLoS One 9: e85879

441 Ferrezuelo F, Colomina N, Palmisano A, Gari E, Gallego C, Csikasz-Nagy A, Aldea M (2012) The critical
442 size is set at a single-cell level by growth rate to attain homeostasis and adaptation. Nat
443 Commun 3: 1012

444 Fingerman I, Nagaraj V, Norris D, Vershon AK (2003) Sfp1 plays a key role in yeast ribosome biogenesis.
445 Eukaryot Cell 2: 1061-8

446 Gomez-Herreros F, de Miguel-Jimenez L, Morillo-Huesca M, Delgado-Ramos L, Munoz-Centeno MC,
447 Chavez S (2012) TFIIS is required for the balanced expression of the genes encoding ribosomal
448 components under transcriptional stress. Nucleic Acids Res 40: 6508-19

449 Harbison CT, Gordon DB, Lee TI, Rinaldi NJ, Macisaac KD, Danford TW, Hannett NM, Tagne JB, Reynolds
450 DB, Yoo J, Jennings EG, Zeitlinger J, Pokholok DK, Kellis M, Rolfe PA, Takusagawa KT, Lander ES,
451 Gifford DK, Fraenkel E, Young RA (2004) Transcriptional regulatory code of a eukaryotic
452 genome. Nature 431: 99-104

453 Haruki H, Nishikawa J, Laemmli UK (2008) The anchor-away technique: rapid, conditional establishment
454 of yeast mutant phenotypes. Molecular cell 31: 925-32

455 Hu B, Petela N, Kurze A, Chan KL, Chapard C, Nasmyth K (2015) Biological chromodynamics: a general
456 method for measuring protein occupancy across the genome by calibrating ChIP-seq. Nucleic
457 Acids Res 43: e132

458 Huber A, French SL, Tekotte H, Yerlikaya S, Stahl M, Perepelkina MP, Tyers M, Rougemont J, Beyer AL,
459 Loewith R (2011) Sch9 regulates ribosome biogenesis via Stb3, Dot6 and Tod6 and the histone
460 deacetylase complex RPD3L. Embo J 30: 3052-64

461 Hughes JD, Estep PW, Tavazoie S, Church GM (2000) Computational identification of cis-regulatory
462 elements associated with groups of functionally related genes in Saccharomyces cerevisiae. J
463 Mol Biol 296: 1205-14

464 Jiang C, Pugh BF (2009) A compiled and systematic reference map of nucleosome positions across the
465 Saccharomyces cerevisiae genome. Genome Biol 10: R109

466 Jorgensen P, Nishikawa JL, Breitkreutz BJ, Tyers M (2002) Systematic identification of pathways that
467 couple cell growth and division in yeast. Science 297: 395-400

468 Jorgensen P, Rupes I, Sharom JR, Schneper L, Broach JR, Tyers M (2004) A dynamic transcriptional
469 network communicates growth potential to ribosome synthesis and critical cell size. Genes
470 Dev 18: 2491-505

471 Jorgensen P, Tyers M (2004) How cells coordinate growth and division. Curr Biol 14: R1014-27

472 Knight B, Kubik S, Ghosh B, Bruzzone MJ, Geertz M, Martin V, Denervaud N, Jacquet P, Ozkan B,
473 Rougemont J, Maerkl SJ, Naef F, Shore D (2014) Two distinct promoter architectures centered
474 on dynamic nucleosomes control ribosomal protein gene transcription. Genes Dev 28: 1695-
475 709

476 Lempiainen H, Shore D (2009) Growth control and ribosome biogenesis. Curr Opin Cell Biol 21: 855-863

477 Lempiainen H, Uotila A, Urban J, Dohnal I, Ammerer G, Loewith R, Shore D (2009) Sfp1 interaction with
478 TORC1 and Mrs6 reveals feedback regulation on TOR signaling. Mol Cell 33: 704-16

479 Liebman SW, Chernoff YO (2012) Prions in yeast. Genetics 191: 1041-72

480 Lippman SI, Broach JR (2009) Protein kinase A and TORC1 activate genes for ribosomal biogenesis by
481 inactivating repressors encoded by Dot6 and its homolog Tod6. Proc Natl Acad Sci U S A 106:
482 19928-33

483 Longtine MS, McKenzie A, 3rd, Demarini DJ, Shah NG, Wach A, Brachat A, Philippsen P, Pringle JR (1998)
484 Additional modules for versatile and economical PCR-based gene deletion and modification in
485 Saccharomyces cerevisiae. Yeast 14: 953-61

486 Marion RM, Regev A, Segal E, Barash Y, Koller D, Friedman N, O'Shea EK (2004) Sfp1 is a stress- and
487 nutrient-sensitive regulator of ribosomal protein gene expression. Proc Natl Acad Sci U S A
488 101: 14315-22

489 Martin DE, Soulard A, Hall MN (2004) TOR Regulates Ribosomal Protein Gene Expression via PKA and
490 the Forkhead Transcription Factor FHL1. Cell 119: 969-79

491 Matveenko AG, Drozdova PB, Belousov MV, Moskalenko SE, Bondarev SA, Barbitoff YA, Nizhnikov AA,
492 Zhouravleva GA (2016) SFP1-mediated prion-dependent lethality is caused by increased Sup35
493 aggregation and alleviated by Sis1. Genes Cells 21: 1290-1308

494 O'Duibhir E, Lijnzaad P, Benschop JJ, Lenstra TL, van Leenen D, Groot Koerkamp MJ, Margaritis T, Brok
495 MO, Kemmeren P, Holstege FC (2014) Cell cycle population effects in perturbation studies.
496 Mol Syst Biol 10: 732

497 Preti M, Ribeyre C, Pascali C, Bosio MC, Cortelazzi B, Rougemont J, Guarnera E, Naef F, Shore D, Dieci G
498 (2010) The telomere-binding protein Tbf1 demarcates snoRNA gene promoters in
499 Saccharomyces cerevisiae. Molecular cell 38: 614-20

500 Reja R, Vinayachandran V, Ghosh S, Pugh BF (2015) Molecular mechanisms of ribosomal protein gene
501 coregulation. Genes Dev 29: 1942-54

502 Rhee HS, Pugh BF (2012) Genome-wide structure and organization of eukaryotic pre-initiation
503 complexes. Nature 483: 295-301

504 Rigaut G, Shevchenko A, Rutz B, Wilm M, Mann M, Seraphin B (1999) A generic protein purification
505 method for protein complex characterization and proteome exploration. Nat Biotechnol 17:
506 1030-1032

507 Rogoza T, Goginashvili A, Rodionova S, Ivanov M, Viktorovskaya O, Rubel A, Volkov K, Mironova L (2010)
508 Non-Mendelian determinant [ISP+] in yeast is a nuclear-residing prion form of the global
509 transcriptional regulator Sfp1. Proc Natl Acad Sci U S A 107: 10573-7

510 Rossi MJ, Lai WKM, Pugh BF (2018) Genome-wide determinants of sequence-specific DNA binding of
511 general regulatory factors. Genome Res 28: 497-508

512 Rudra D, Zhao Y, Warner JR (2005) Central role of Ifh1p-Fhl1p interaction in the synthesis of yeast
513 ribosomal proteins. Embo J 24: 533-42

514 Schawalder SB, Kabani M, Howald I, Choudhury U, Werner M, Shore D (2004) Growth-regulated
515 recruitment of the essential yeast ribosomal protein gene activator Ifh1. Nature 432: 1058-61

516 Schmid M, Durussel T, Laemmli UK (2004) ChIC and ChEC; genomic mapping of chromatin proteins. Mol
517 Cell 16: 147-57

518 Singh J, Tyers M (2009) A Rab escort protein integrates the secretion system with TOR signaling and
519 ribosome biogenesis. Genes Dev 23: 1944-58

520 Skene PJ, Henikoff S (2015) A simple method for generating high-resolution maps of genome-wide
521 protein binding. Elife 4: e09225

522 Sun M, Schwalb B, Schulz D, Pirkl N, Etzold S, Lariviere L, Maier KC, Seizl M, Tresch A, Cramer P (2012)
523 Comparative dynamic transcriptome analysis (cDTA) reveals mutual feedback between mRNA
524 synthesis and degradation. Genome Res 22: 1350-9

525 Tokiwa G, Tyers M, Volpe T, Futcher B (1994) Inhibition of G1 cyclin activity by the Ras/cAMP pathway
526 in yeast. Nature 371: 342-5

527 Volkov KV, Aksenova AY, Soom MJ, Osipov KV, Svitin AV, Kurischko C, Shkundina IS, Ter-Avanesyan MD,
528 Inge-Vechtomov SG, Mironova LN (2002) Novel non-Mendelian determinant involved in the
529 control of translation accuracy in Saccharomyces cerevisiae. Genetics 160: 25-36

530 Wade JT, Hall DB, Struhl K (2004) The transcription factor Ifh1 is a key regulator of yeast ribosomal
531 protein genes. Nature 432: 1054-8

532 Warner JR (1999) The economics of ribosome biosynthesis in yeast. Trends Biochem Sci 24: 437-40

533 Xu Z, Norris D (1998) The SFP1 gene product of Saccharomyces cerevisiae regulates G2/M transitions
534 during the mitotic cell cycle and DNA-damage response. Genetics 150: 1419-28

535 Zentner GE, Kasinathan S, Xin B, Rohs R, Henikoff S (2015) ChEC-seq kinetics discriminates transcription
536 factor binding sites by DNA sequence and shape in vivo. Nat Commun 6: 8733

537 Zhu C, Byers KJ, McCord RP, Shi Z, Berger MF, Newburger DE, Saulrieta K, Smith Z, Shah MV,
538 Radhakrishnan M, Philippakis AA, Hu Y, De Masi F, Pacek M, Rolfs A, Murthy T, Labaer J, Bulyk
539 ML (2009) High-resolution DNA-binding specificity analysis of yeast transcription factors.
540 Genome Res 19: 556-66

541

542 ## Acknowledgements

543 We thank other members of the Shore laboratory for helpful discussions; Florian Steiner and Robbie
544 Loewith for comments on the manuscript; Uli Laemmli for ChEC reagents and advice on the ChEC
545 method; Mylène Docquier and the Institute of Genetics and Genomics of Geneva (iGE3;
546 http://www.ige3.unige.ch/genomics-platform.php) for high-throughput DNA sequencing; Nicolas
547 Roggli for expert artwork; and Thomas Schalch for the use of his local Galaxy server. B.A. acknowledges
548 support from an EMBO Long-Term Fellowship. D.S. acknowledges support from the Swiss National
549 Fund (grant number 31003A_170153) and the Republic and Canton of Geneva.

550

551 ## Author contributions

552 B.A. and S.T. designed the study, together with D.S., and carried out most of the experiments. Y.G.
553 constructed and characterized Sfp1 anchor-away strains, B.A. and S.M. performed all ChEC-seq
554 experiments, and S.K. analysed RNAPII binding on coding regions and the "spike-in" control for RNAPII
555 ChIP-seq following Sfp1 depletion. B.A. and D.S. wrote the manuscript.

556

557 ## Competing interests

558 The authors declare no competing interests.

559